ELSEVIER

Clinical Neurophysiology 114 (2003) 2107–2117

www.elsevier.com/locate/clinph

Muscle afferent inputs from the hand activate human cerebellum sequentially through parallel and climbing fiber systems

Isao Hashimoto[a,c,*], Tomoaki Kimura[b], Masato Tanosaki[c], Yoshinobu Iguchi[c], Kensuke Sekihara[d]

[a]*Human Information Systems Laboratory, Tokyo Office, Kanazawa Institute of Technology, 6-8-7 Akasaka, Minato-ku, Tokyo 107-0052, Japan*
[b]*Department of Acupuncture, Tsukuba College of Technology, Tsukuba, Japan*
[c]*Department of Integrated Neuroscience, Tokyo Institute of Psychiatry, Tokyo, Japan*
[d]*Department of Electronic Systems and Engineering, Tokyo Metropolitan Institute of Technology, Tokyo, Japan*

Accepted 11 June 2003

Abstract

Objective: Spatio-temporal response characteristics of the human cerebellum to median nerve stimulation (MNS) were studied with the use of a whole-head magnetoencephalographic (MEG) system covering the cerebellum and upper cervical spine.

Methods: Neuromagnetic responses from the cerebellum were recorded following electric stimulation of the right median nerve in 12 subjects. In 6 out of 12 subjects, the responses to the left median nerve and to the right index or middle finger stimulation were also recorded.

Results: The medial part of the cerebellum (spinocerebellum) was activated by MNS. In contrast, there were no responses from the cerebellum to the finger stimulation, suggesting that muscle afferent inputs are the source of cerebellar activation for MNS. The cerebellar responses consisted of 3 or 4 components of alternating polarity within 90 ms post-stimulus: the current direction for the first component was from the depth to the surface of the anterior lobe.

Conclusions: From the timing and current direction, we speculate that the 4 components reflect, respectively, (1) excitatory postsynaptic potentials (EPSPs) of granule cells, (2) Purkinje cell EPSPs at the distal dendrites driven by parallel fibers, (3) Purkinje cell EPSPs at the soma and the proximal dendrites mediated by climbing fibers and (4) second Purkinje cell EPSPs at the distal dendrites driven by parallel fibers.

Significance: We first visualized serial activation of the human spinocerebellum following MNS noninvasively with MEG.

Keywords: Magnetoencephalography; Muscle afferent input; Cerebellum; Granule cell; Purkinje cell; Parallel fiber system; Climbing fiber system

1. Introduction

Noninvasive neuroimaging techniques such as positron emission tomography (PET) and functional magnetic resonance imaging (fMRI) have shown repeatedly that voluntary movements of the hand activate the vermal and intermediate zone (spinocerebellum) of ipsilateral anterior lobe of human cerebellum (Grafton et al., 1993; Ellerman et al., 1994; Nitschke et al., 1996; Sakai et al., 1998; Grodd et al., 2001). On the other hand, although the temporal relations between activities of the spinocerebellum and various aspects of hand movements were extensively studied electrophysiologically in animals, the input-output timing relations still remained obscure (Harvey et al., 1977; Thach, 1978; Van Kan et al., 1993a,b; see Ghez and Thach, 2000 for review). As a first step toward elucidating a complex neural-behavioral coupling, we aimed to characterize the spatio-temporal patterns of the cerebellar activation in humans to median nerve stimulation (MNS). Specifically, the timing of mossy fiber activation of granule cells and the timing of parallel and climbing fiber system activation of Purkinje cells with respect to peripheral inputs are crucial for understanding the underlying physiological mechanisms of monitoring and adjusting on-going movements in humans.

Tesche and Karhu (1997, 2000) were able to extract a short-latency response or sustained oscillatory activity in the human cerebellum to MNS on a priori assumption that

* Corresponding author. Tel.: +81-3-5545-8197; fax: +81-3-5545-8199.
E-mail address: ihashi@ael.kanazawa-it.ac.jp (I. Hashimoto).

1388-2457/$30.00
doi:10.1016/S1388-2457(03)00233-5

an equivalent current dipole (ECD) exists in the human cerebellum. Except for the reports above, no electroencephalographic (EEG) or magnetoencephalographic (MEG) observations of human cerebellar activity to somatosensory stimulation appear in the literature. There are 3 main reasons for the difficulty in the noninvasive physiological detection of the cerebellar activity. First, extensive cortical foliation and diverse branching of the dendritic trees of Purkinje cells in the macro- and microstructure of the cerebellar cortex are clearly less than optimal for generating an 'open' electric field (Lorente de No, 1947). Second, the cerebellum is located fairly deep within the cranium; it is closer to the center of the sphere than to the surface. Third, the previous commercially available whole-head MEG systems were designed for recording cerebral activity and not for recording cerebellar activity. In this situation, what we can do to detect the magnetic signals from the cerebellum is first to use a whole-head MEG system covering not only the cerebrum but also the cerebellum and second to increase the signal-to-noise ratio. Thus, we used a new MEG system covering both cerebrum and cerebellum and averaged a massive number of 10 000 epochs in the present study.

We estimated the source of magnetic signals to MNS with a single dipole modeling in a small number of subjects. This approach, however, was not successful in locating the cerebellar source in more than half of the subjects mainly because of contamination by overwhelmingly strong parallel cerebral responses. The issue has been complicated further when the source localization for the activity of relatively wide areas of human cerebellum is to be estimated using a single dipole model.

The adaptive vector beamformer technique recently developed by Sekihara et al. (2001) has provided us with a unique tool for the analysis of multiple sources located nearby in primary somatosensory cortex (SI), which are activated in parallel or successively (Hashimoto et al., 2001a,b). In the present study, we used this beamformer technique and showed that the robust cerebellar activation can be visualized at the latency range of 15–90 ms following MNS.

2. Materials and methods

Twelve normal subjects (2 females, 10 males, aged 22–34 years, mean 25.6) were studied during wakefulness. All subjects were right-handed according to the Edinburgh inventory (Oldfield, 1971) and written informed consent was obtained before the experiments. All experimental protocols were conducted in accordance with the Declaration of Helsinki and were approved by the Institutional Bioethics Committee of Tokyo Institute of Psychiatry.

Constant current pulses (rectangular shape, 0.2 ms duration) were delivered at a stimulus rate of 4 Hz to the right median nerve at the wrist in 12 subjects and also to the left median nerve in 6 out of 12 subjects. In 6 out of 12 subjects, the stimuli were delivered to the index (in 2 subjects) or middle finger (in 4 subjects) via a pair of ring electrodes with the cathode and anode placed at the proximal interphalangeal and distal interphalangeal joint, respectively. The stimulus intensity was 3 times sensory threshold for the median nerve and finger stimulation. This stimulus intensity elicited a mild twitch of the abductor pollicis brevis muscle for MNS.

Magnetic signals (bandpass 3–2000 Hz) were recorded in a magnetically shielded room using a 160-channel whole-head type gradiometer system (Yokogawa MEGVISION, Yokogawa Electric Corp., Tokyo). The detection coils of the gradiometer are arranged in a uniform array on a helmet-shaped surface of the bottom of the dewar, and the distance between the centers of two adjacent coils is 25 mm; each coil measures 15.5 mm in diameter. The sensor array covers not only the cerebrum but also the cerebellum and upper cervical spine (Fig. 1). The sensors are configured as first-order axial gradiometers with a baseline of 50 mm. The field sensitivities

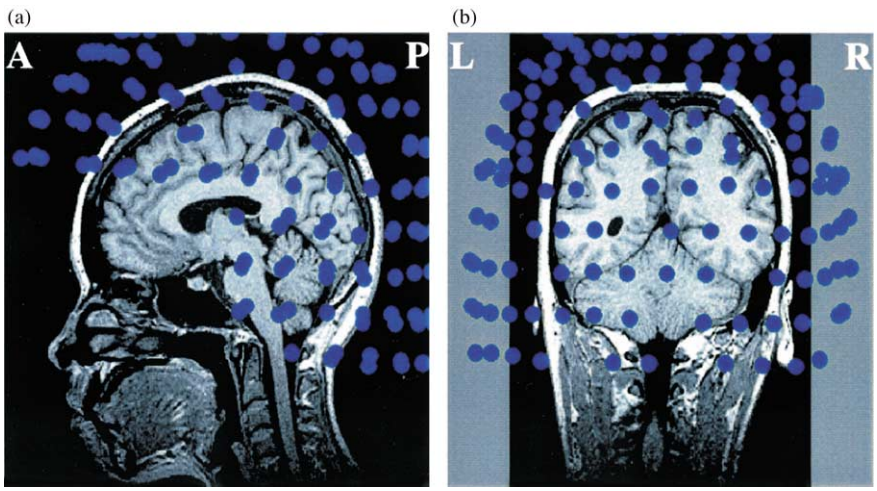

Fig. 1. Sensor array superimposed on MRI in a subject. Note complete coverage of the cerebellum by the sensors.

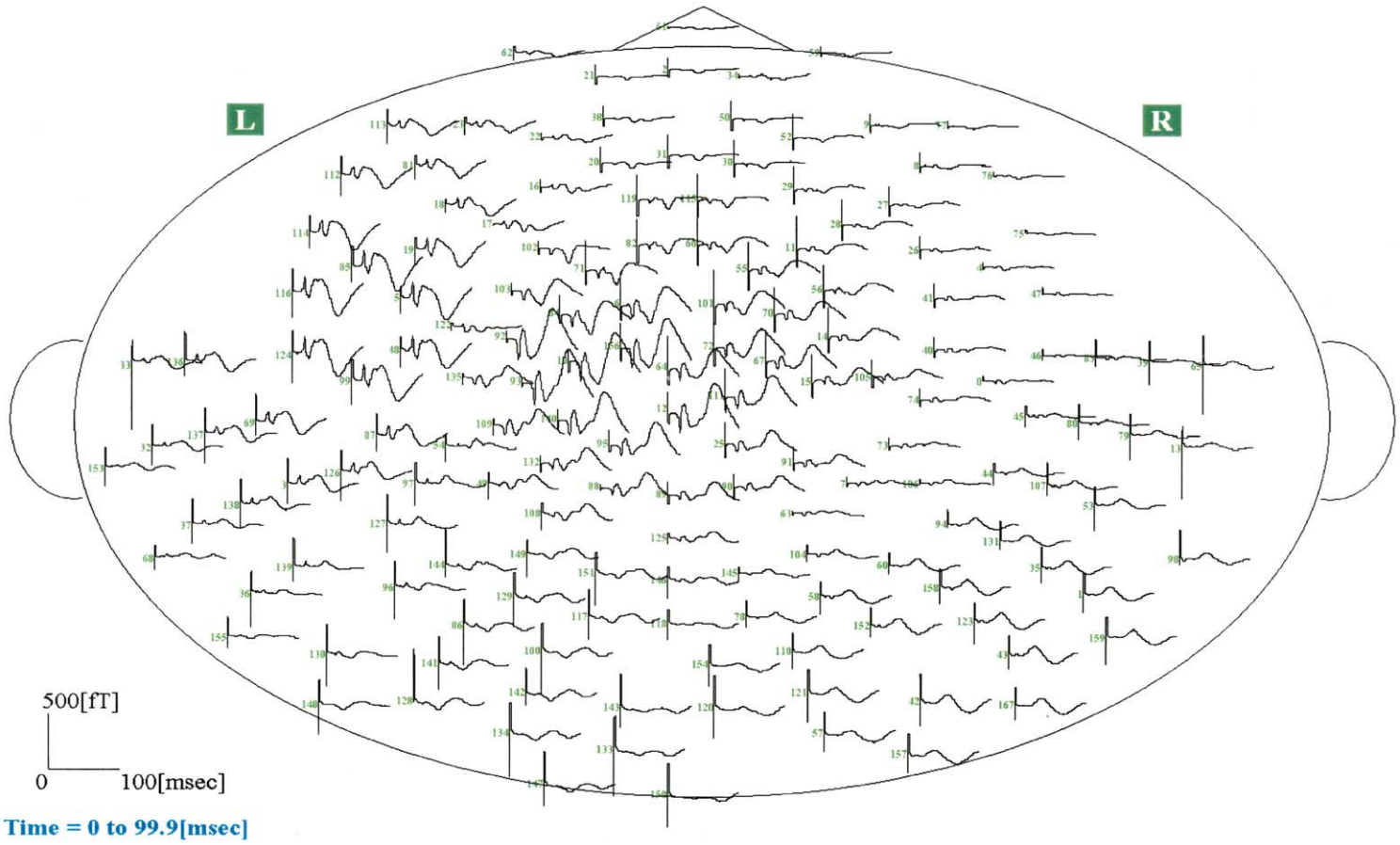

Fig. 2. Somatosensory evoked fields (SEFs) from 160 channels following right median nerve stimulation (MNS) in a representative subject are displayed at the approximate locations of the sensors. The time window ranges from 0 to100 ms after MNS. Top view with nose up. The letters R and L indicate right and left hemispheres, respectively.

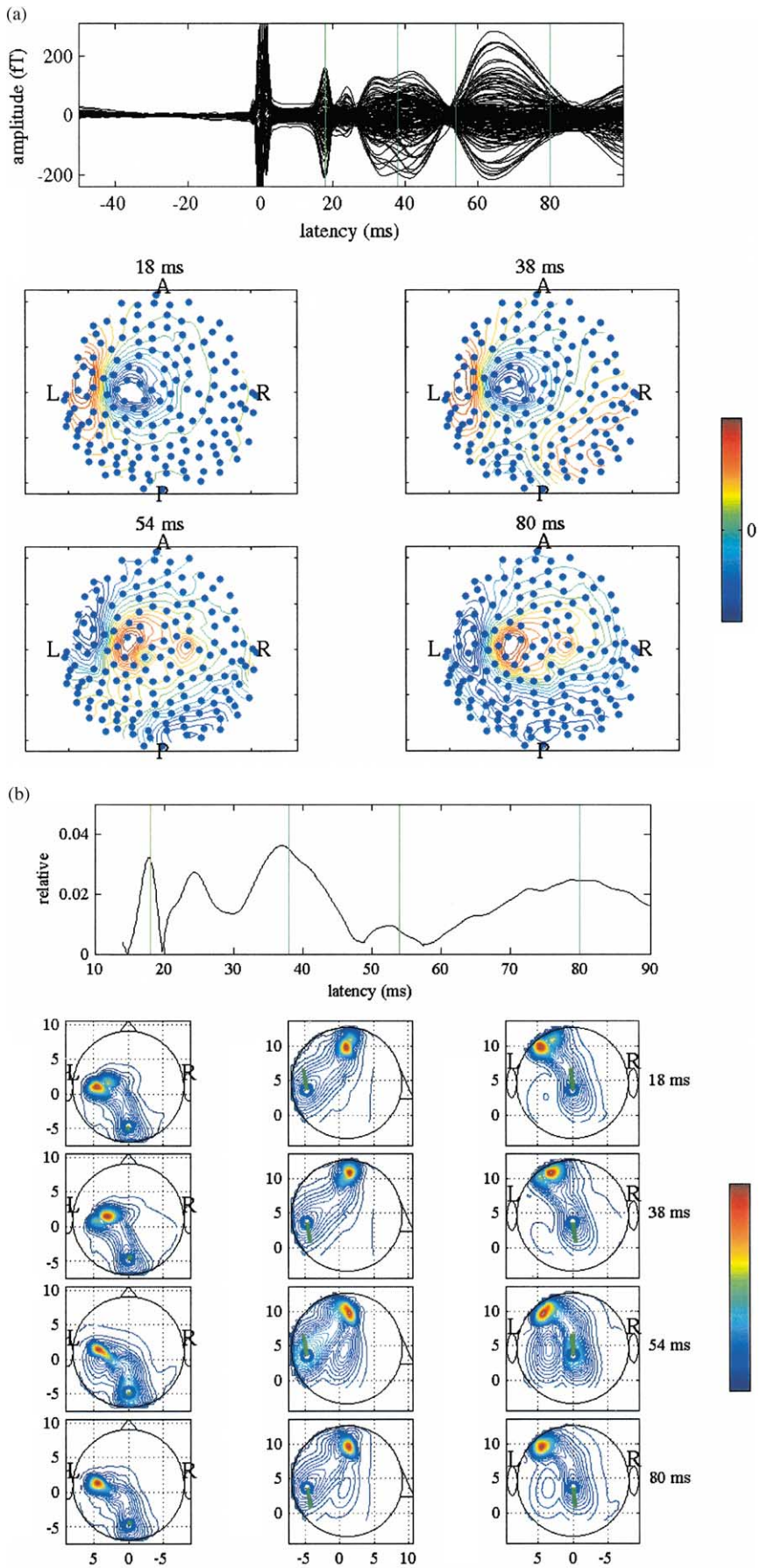
(a)
amplitude (fT)
200
0
-200
-40
-20
0
20
40
60
80
latency (ms)
18 ms
38 ms
54 ms
80 ms
A
L
R
P
0
(b)
relative
0.04
0.02
0
10
20
30
40
50
60
70
80
90
latency (ms)
18 ms
38 ms
54 ms
80 ms

of the sensors were 5 fT/$\sqrt{\text{Hz}}$ or better. An epoch of 150 ms duration (50 ms pre- and 100 ms post-stimulus) was digitized at a 10 kHz/channel sampling rate and 10 000 responses were averaged on-line. DC offset was based on the pre-stimulus period. The wide-band recorded responses were digitally filtered with a bandpass of 3–300 Hz.

Magnetic resonance imaging (MRI) scans (Magnetom System, Symphony 1.5 T, Siemens, 1.0 mm thickness) were acquired with spherical lipid markers placed on the 5 MEG fiduciary points to allow superposition of magnetic source locations onto the MRI slices. The MRI head shape data were used to determine the best-fit sphere for each subject's head. The head coordinate was defined as follows. The origin was defined as the midpoint between the pre-auricular points. The x-axis passed from the origin to the nasion. The y-axis was adjusted to be perpendicular to the x-axis on the plane made by the nasion and pre-auricular points, with positive direction to the left. The z-axis pointed to the vertex in a direction perpendicular to the x-y plane.

2.1. Data analysis

By using the adaptive vector beamformer technique, the source localization was performed from the whole data set between the period of 10 and 90 ms post-stimulus. The results of the analysis were shown as maximum intensity projections of current density for transverse, sagittal and coronal sections of the generic head. The details of this adaptive vector beamformer technique and its application to SEF data were reported previously (Sekihara et al., 2001; Hashimoto et al., 2001a,b). Therefore, it is only briefly described here.

Let us define the magnetic field measured by the mth sensor at time t as $b_m(t)$, and a column vector $\mathbf{b}(t) = [b_1(t), \ldots, b_M(t)]^T$ as a set of measured data. Here M is the total number of sensors and the superscript T indicates the matrix transpose. A spatial location (x, y, z) is represented by a 3-dimensional vector $\mathbf{r} : \mathbf{r} = (x, y, z)$. The source moment magnitude at $\mathbf{r}$ and time t is defined as a 3-dimensional vector $\mathbf{s}(\mathbf{r}, t) = [s_x(\mathbf{r}, t), s_y(\mathbf{r}, t), s_z(\mathbf{r}, t)]$. The estimate of the source moment is denoted as $\hat{\mathbf{s}}(\mathbf{r}, t)$. We define the lead field matrix $\mathbf{L}(\mathbf{r})$ that represents the sensitivity of the whole sensor array at $\mathbf{r}$.

The vector beamformer technique reconstructs the source moment by applying the following linear operation.

$$\hat{\mathbf{s}}(\mathbf{r}, t) = \mathbf{W}^T(\mathbf{r})\mathbf{b}(t) \tag{1}$$

where the matrix $\mathbf{W}(\mathbf{r})$ is a weight matrix defined in Eq. (9) in the literature (Sekihara et al., 2001). Then, the source moment at the location $\mathbf{r}$ is estimated using Eq. (1). Note that when calculating the above weight matrix, the location $\mathbf{r}$ is a controllable parameter. Therefore, the source-moment distribution can be reconstructed by scanning the beamformer output over the region of interest in a completely post-processing manner. Because this reconstruction is performed at each instant in time, the spatio-temporal reconstruction of the source activities can be obtained.

It should be emphasized that the adaptive beamformer technique described above does not require any such prior assumptions on the source configuration as the source location, the source orientation, or the number of sources. In this technique, the spatial resolution depends on the input SNR, which is proportional to $\sigma^2\|\mathbf{L}(\mathbf{r})\|^2$ where σ^2 is the source power and $\|\mathbf{L}(\mathbf{r})\|^2$ is the square of the lead-field norm. Since the square of the lead-field norm is inversely proportional to the fourth power of the source depth, a deep source has a spatial resolution lower than that for a shallow source. Considering the average distance between a source and sensors, the spatial resolution is approximately estimated to be 1 cm for a source in the SI region, whereas it is estimated to be 2–2.5 cm for a source in the cerebellar region (Sekihara et al., 2002).

3. Results

The primary N20m deflection was clearly identified in somatosensory evoked fields (SEFs) following MNS in all subjects. In Fig. 2, the raw waveform data were displayed at the approximate locations of the sensors. The isofield contour maps around N20m peak at the latency of 18 ms demonstrated a clear polarity reversal over the left 3b hand area to right MNS, indicating that the N20m can be approximated by a single dipole (Fig. 3a). The time course and the current-density maps of the typical cerebellar activation are illustrated in Fig. 3b. The current-density map

Fig. 3. (a) Somatosensory evoked fields (SEFs) from 160 channels following right median nerve stimulation (MNS) are superimposed at the top. Four isofield contour maps at the latencies indicated on top of each map are shown. The colors of the contours represent the relative intensity of the magnetic field as indicated by the color bar. Vertical green lines on the superimposed traces indicate the selected time points for the maps. In addition to a dipolar pattern over the left primary somatosensory cortex (SI), another dipolar pattern is clearly seen over the cerebellum at 38 ms post-stimulus. (b) Time-course of the cerebellar activation and current density maps at the latencies of the isofield contour maps in (a). In addition to the SI source, cerebellar activation is shown at all latencies indicted on the right of the maps. The 4 vertical lines on the time course of cerebellar activation also indicate these latencies. In each row, the maximum-intensity projections onto the axial (left), sagittal (middle), and coronal (right) directions are shown. The circles depicting a human head show the projections of the sphere used for the forward modeling. The colors of the contours represent the relative intensity of the source magnitude as indicated by the color bar. The coordinate is the head coordinate expressed in cm. The small green bars originating from the center of the sources indicate the moment directions of these sources. The letters R and L in the axial and coronal views indicate right and left hemispheres, respectively. Note that the source is stationary throughout, and only the direction of the current changes from the first (18 ms) to the second (38 ms) component, from the second to the third (54 ms) and from the third to the fourth (80 ms) component.

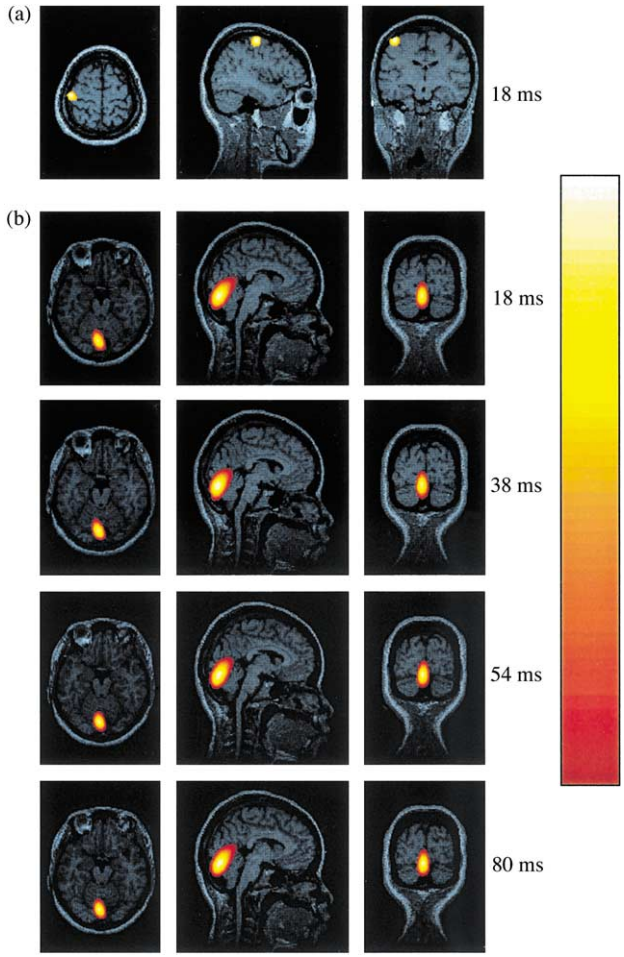

Fig. 4. Superimposition of SI and cerebellar sources onto the subject's MRI for the data presented in Fig. 2. From the left to right columns are axial, sagittal and coronal sections of the MRI. SI source at 18 ms post-stimulus (a) and 4 cerebellar sources (b) are shown. Here, the source intensities above a certain threshold are color coded according to the color bar at the right and overlaid onto the subject MRI.

at the peak of N20m revealed initial activation of SI. The first response with a relatively short duration at the latency of 18 ms was observed over the cerebellum in parallel with the N20m SI response (Fig. 3b). This component had the moment direction from inferior to superior. The second cerebellar response with the current direction toward inferior appeared at the latency of 38 ms, in addition to the SI dipole (Fig. 3a,b). The dipolar pattern over the cerebellum is clearly seen at this time slice (Fig. 3a). The third response with the same current direction as for the first response occurred at the latency of 54 ms (Fig. 3b). Finally, the fourth response with the same current direction as for the second response appeared at 80 ms post-stimulus (Fig. 3b). Co-registration of the MEG sources onto the subject's MRI showed that the left SI and the medial zone of the cerebellum were activated at each time-slice following the right MNS (Fig. 4). In this figure, the cerebellar sources are somewhat diffuse, and considerably large regions look activated. However, this diffuse appearance of activation was caused by the fact that the spatial resolution of the adaptive beamformer technique is relatively low in a deep area such as the cerebellar region (Sekihara et al., 2002).

We were able to determine the locations and orientations of the cerebellar sources in 7 out of 12 subjects for right

Table 1
Latency (ms) of transit (T) from the first (T1) to fourth (T4) cerebellar components

Stimulus	T1–2	T2–3	T3–4
Right	36.0 ± 9.9	59.4 ± 14.4	67.0 ± 8.5
Left	28.3 ± 9.0	46.8 ± 15.7	68.5 ± 19.8
Total	31.8 ± 9.8	52.5 ± 15.7	68.1 ± 17.1

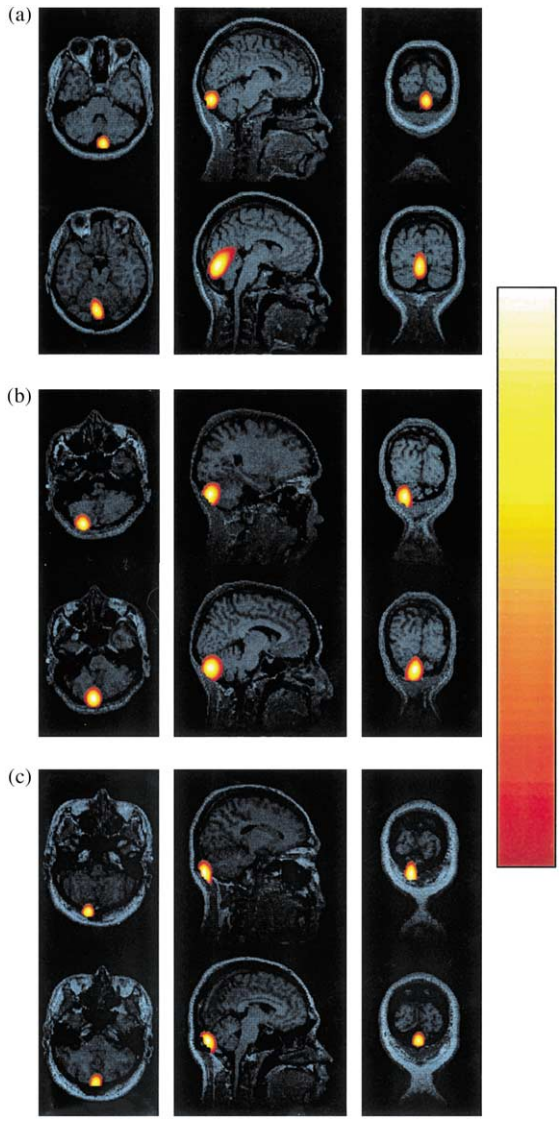

Fig. 5. Superimposition of the first cerebellar source onto each subject's MRI in 3 subjects (a, b and c). From the left to right columns are axial, sagittal and coronal sections of the MRI. Here, the source intensities above a certain threshold are color coded according to the color bar at the right and overlaid onto the subject MRI. For each subject, upper row illustrates activation for left MNS and lower row activation for right MNS.

MNS and in 5 out of 6 subjects for left MNS. Since the peak latency of each cerebellar component was difficult to define, we measured the latency of polarity reversal: the transit from the first component into the second component, and from the second into the third, and from the third into the fourth, respectively (Table 1). Although there were considerable variations in the latency of the transitions across subjects, the mean duration was about 15–30 ms for the first response, 30–50 ms for the second, 50–70 ms for the third and > 70 ms for the fourth response.

For each subject, the initial 3 or 4 sources were located close with each other in the medial part of the cerebellum mainly ipsilateral to the stimulus. The mean locations of the first source for 3 subjects were overlaid on each subject's MRI in Fig. 5. Here, again the cerebellar sources look considerably diffused due to the low spatial resolution of the source reconstruction technique. In addition, the source was localized slightly outside the border of the cerebellum for the third subject (Fig. 5c). This is probably because the use of a spherically homogeneous conductor model for the forward modeling might cause small inaccuracy and the source is localized closer to the surface than the actual locations.

The locations of the maximum points of cerebellar sources in 5 subjects for left MNS and in 7 subjects for right MNS were schematically illustrated in Fig. 6. For the left MNS, the sources were clustered in the medial zone mainly ipsilateral to the stimulus. For the right MNS, the sources were somewhat scattered around the midline of the cerebellum.

The first cerebellar source was concurrent with the N20m SI source and the current direction was from inferior to superior. Given the magnetic source in the cerebellar cortex of the anterior lobe demonstrated in fMRI studies (see Sections 1 and 4), it follows that an algebraic sum of the intracellular current is from the depth to the surface of the cerebellar cortex, indicating the depth-sink and the surface-source configuration of the field potential. This current direction for the first source was consistent for all subjects. For the second source, the direction was from the surface to the depth, reflecting the surface-sink and the depth-source configuration. For the third source, the direction was from the depth to the surface in all subjects. For the fourth source, the direction was from the surface to the depth.

Finally, for all 6 subjects studied, SI responses were recorded from the cerebral cortex to the index or middle finger stimulation. However, no responses from the cerebellum were observed, thus suggesting the possibility that contribution from skin afferent inputs can be eliminated.

4. Discussion

The present results show that cerebellar SEFs can be detected, without any anatomical or physiological constraints, by the whole-head axial gradiometer covering the cerebellum and that the activation of cerebellar source areas can be identified.

4.1. Muscle afferent inputs are the source of cerebellar activation

In sharp contrast with the median nerve SEFs, there were no responses from the cerebellum to the index or middle finger stimulation, thus suggesting that contribution from skin afferent inputs to the cerebellar responses can be ruled out. Since median nerve is a mixed nerve consisting of skin and muscle afferent fibers, it is reasonable to conclude that muscle afferent inputs are the source of the cerebellar activation. The source areas in MEG recordings for MNS

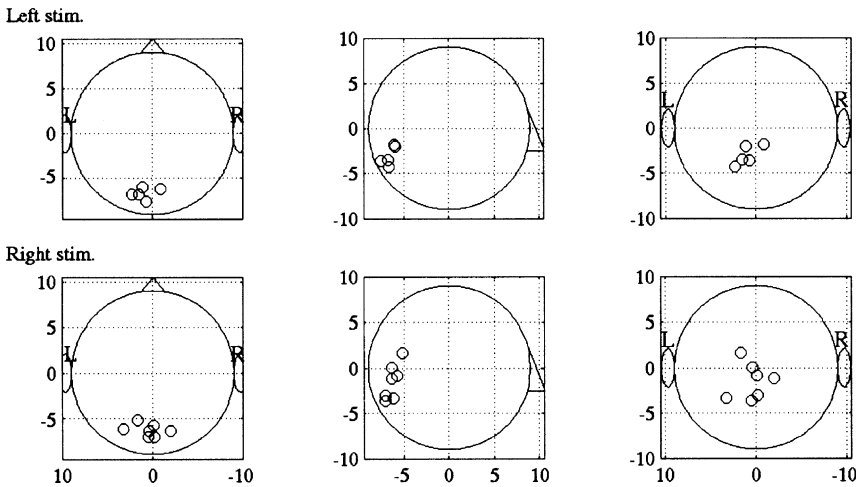

Fig. 6. Schematic illustration of the locations of cerebellar sources. Open circles show locations of cerebellar source in each subject for left MNS (top row) and for right MNS (bottom row). These locations were obtained as the locations of the maximum points of the cerebellar activations. In each row, the locations onto the axial (left), sagittal (middle) and coronal (left) directions are shown. The letters R and L in the axial and coronal views indicate right and left hemispheres, respectively.

are in line with PET and fMRI studies that voluntary movements of the hand activate the vermal and intermediate zone of ipsilateral anterior lobe of human cerebellum (Grafton et al., 1993; Ellerman et al., 1994; Nitschke et al., 1996; Sakai et al., 1998; Grodd et al., 2001). It may be argued however that the failure to observe responses with finger stimulation simply reflects a smaller number of afferent fibers activated by the finger stimulation and/or the lack of sensitivity of the MEG imaging technique, since somatosensory information from the skin reaches the cerebellar cortex via a variety of pathways in animals (Oscarsson, 1973; Harvey et al., 1977; Rushmer et al., 1980). This may not be the case because we showed repeatedly in our previous studies that the amplitude of the cerebral responses is not always linearly related to the number of activated fibers per se (see for example Hashimoto et al., 1990). This non-linearity in the responses in the cerebral cortex may also apply to those in the cerebellar cortex. However, it is worthwhile to examine the above possibility by stimulating the superficial radial nerve or multiple fingers simultaneously to increase the number of fibers activated. We are planning to address this issue systematically to confirm the present results in a future study.

There is another possibility that cutaneous receptors are activated as a result of limb movements and the cutaneous inputs might be also transmitted to the cerebellum. A microneurographic study clearly shows that cutaneous mechanoreceptors in the dorsum of the human hand respond to hand or finger movements and provide the CNS with detailed kinematic information for movements of the hand (Edin and Abbs, 1991). Thus it is possible that not only muscle afferents but also cutaneous afferents contribute to the cerebellar responses. However, the cutaneous afferent contribution to the cerebellar responses may be minimal, if any, because pure cutaneous inputs with electric finger stimulation elicit no detectable responses from the cerebellum. In support of this conjecture, cerebellar activation is hard to detect in humans during tactile stimulation and there has been only one fMRI study showing activation of the cerebellum to tactile stimulation of hand and foot (Bushara et al., 2001). Thus, further studies are needed to clarify the discrepancy between the present study and electrophysiological studies in animals or the fMRI study in man.

4.2. The first cerebellar response reflects activity in the granule cells

The first response with a short duration at the latency of 15–30 ms was observed over the medial zone of the anterior lobe. Because fast mossy fibers from the external cuneate nucleus activate granule cells at the shortest latency (Oscarsson, 1973; Murphy et al., 1973), the population of granule cells is the most probable candidate for the initial response. It was also shown that stimulation of the external cuneate nucleus or the dorsal spinocerebellar tract evoked postsynaptic currents in the granule cells in the form of N_2 field potential (Sasaki and Strata, 1967). The depth profile of this field potential showed the maximum negativity in the granular layer, which fell off toward the superficial molecular layer. The direction of the current for the first cerebellar source was from the depth to the surface of the anterior lobe of the cerebellum and was in agreement with its source in the granule cells. It is well established that the mossy fiber-granule cell system occupies as much as two thirds of the whole cerebellar mass and a large number of the granule cells are activated simultaneously by the cuneocerebellar inputs (Ito, 1984). The first cerebellar response in humans, therefore, may reflect the N_2 potential representing the short-latency excitatory postsynaptic potentials (EPSPs) of granule cells.

Axonal volleys at 13 and 14 ms with duration of 1 ms and a postsynaptic activity at 15 ms with duration of 6 ms were recorded directly from the human dorsal pons and midbrain following MNS (Hashimoto, 1984). These local potentials are detected as P13 and P14 far-field potentials and as N15 potential at the scalp. The sharp P13 and P14 potentials reflect the earliest medial lemniscus volleys, and the slow N15 potential in the pons and midbrain represents excitation of various brain-stem nuclei receiving projections from the cuneate nucleus. The P13 and P14 also elicit postsynaptic P16 in the thalamus (Katayama and Tsubokawa, 1987; Morioka et al., 1989; Klostermann et al., 2002). Thus, if we compare the earliest response in the brain-stem and cerebellum, the brain-stem potentials were earlier than the first cerebellar activation, supporting the notion that the granule cells are the generator for the first cerebellar response.

On the other hand, there is a slower component generated in the brain-stem: widespread N18 component over the scalp, according to Sonoo et al. (1992, 1999), reflects primary afferent depolarization (PAD) of the presynaptic terminals in the cuneate nucleus. The PAD, i.e. EPSPs of the presynaptic terminals of the dorsal column fibers is produced disynaptically by activation of interneurons via collaterals of cuneate neurons. This slow rising and decaying response persists when the earliest activity ascends, passes the brain-stem nuclei and thalamus, and even after it reaches the cortex. Because of a similar timing between N18 and the initial cerebellar response, one may argue that the first ‘cerebellar activation’ reflects postsynaptic activity of the cuneate nucleus. This possibility seems to be slim, because there is a relatively wide distance between the two structures. In addition, the activity of the brain-stem, located deeper than the cerebellum, is much harder to detect with our new gradiometer system with a baseline of 5 cm.

4.3. Purkinje cells are the major generator of the following cerebellar responses

Purkinje cell dendrites in the cerebellar fissures and gyri produce a coherent intracellular current flow and may

generate magnetic fields that can be detectable over the cerebellum. Okada et al. (1987) and Okada and Nicholson (1988) recorded magnetic fields from an isolated turtle cerebellum to electric stimulation of the cerebellar surface. Based on the field pattern, they ascribed the magnetic fields to postsynaptic intracellular current flow in Purkinje cell dendrites. They also showed that a synchronous activity in a 1 mm^3 of in vitro cerebellar tissue could lead to a magnetic field of 100 f T at a distance of 2 cm (Okada et al., 1987). An fMRI study for thumb movements showed an activation volume of 2100 mm^3 in the cerebellum (Grodd et al., 2001). Assuming that the similar volume is activated synchronously for MNS as for thumb movements, a magnetic field of 210 pT at a distance of 2 cm will be produced. However, in vivo responses from the human cerebellum may be considerably reduced because of (1) cancellation of magnetic fields due to a complex macro- and microstructure of the cerebellar folia, (2) a sharp decay in field strength due to its deep location within the cranium, and (3) temporal dispersion due to less coherent activation as shown in the present study. Although no cerebellar responses were observed in 5 out of 12 subjects for right MNS and in 1 out of 6 subjects for left MNS, the present results suggest that cerebellar activity can be detected in the majority of cases. The robustness of our observations argues against the traditional concept of a 'closed' electric field for cerebellar activity, and suggests that there is some systematic asymmetry in the cerebellar structure that produces a 'semi-open' electric field. In fact, the amplitude of the second and third cerebellar responses was on the order of the amplitude of the N20m primary response in SI. However, in subjects without observable cerebellar responses to MNS, it is likely that the 'systematic asymmetry' in the anatomical structure is lost, which produces a closed electric field.

About the functions of the cerebellum, there is growing evidence that the cerebellum might filter out predictable aspects of the sensory input to reveal the unexpected (Bell, 2001). It is tempting to speculate that, through the process of extensive averaging of responses to the rhythmic 4 Hz stimuli, the cerebellar responses have been filtered out. And, as a result, no responses were detected in some of our subjects.

4.4. The second cerebellar activation reflects Purkinje cell EPSPs at the distal dendrites driven by the parallel fibers

The second activation occurred at the latency of 30–50 ms and the current direction of this source was from the cerebellar surface of the anterior lobe toward the depth, reflecting the surface-sink and the depth-source configuration of the field potentials. As the parallel fiber excitatory synapses are concentrated on the most superficial dendritic branches of the Purkinje cells, the distal dendrites become sinks for extracellular return current from the passive sources on the deeper dendrites (Eccles et al., 1966a). The latencies of Purkinje cell responses in cats are 3–4 ms longer than those of granule cells in the immediate vicinity (Murphy et al., 1973). Consideration of the current direction and timing in human and animal studies suggests that the second activation reflects the Purkinje cell activity in the spinocerebellum elicited by the parallel fiber system.

Proprioceptive inputs carried over parallel fiber pathways produce narrow beams of pure inhibition of Purkinje cells (off-beam) on either side of a wide zone of excitation (on-beam) along the transverse axis of the folia (Ito, 1984). However, only 3% of Purkinje cells were inhibited by the proprioceptive inputs (Murphy et al., 1973), suggesting that proprioceptive inputs via the parallel fibers elicit mainly excitatory response.

4.5. The third cerebellar activation reflects Purkinje cell EPSPs at the proximal dendrites mediated by the climbing fibers

The third cerebellar activation occurred at the latency of 50–70 ms and the direction of the current was from the depth to the surface, indicating the depth-sink and the surface-source configuration. The third activation appears to be through the climbing fiber system, because the climbing fibers terminate on the soma and proximal dendrites of the Purkinje cells and produce the current sink at the depth and the source at the surface. The mass activity in the Purkinje cells to climbing fiber stimulation can be recorded as a negative potential in the Purkinje cell and molecular layers and as a positive potential at the cerebellar surface (Eccles et al., 1966b, 1968; Oscarsson, 1973). In addition, the sequential timing of the second and third responses is concordant with electrophysiology of the cerebellum in animals that the conduction velocity for the parallel fibers is faster than for the climbing fibers, and also the latency for the parallel fiber activation of Purkinje cells is shorter than for the climbing fiber mediated Purkinje cell responses (Eccles et al., 1968; Oscarsson, 1973; Murphy et al., 1973).

Oscarsson (1973) has outlined the pertinent pathways through the spinal cord and the inferior olive to the cerebellum (spino-olivo-cerebellar pathways) that mediate the climbing fiber responses. Among 3 physiologically defined climbing fiber pathways, the dorsal spino-olivo-cerebellar pathway transmits the muscle afferent information to the Purkinje cells in the vermis and intermediate part of the anterior lobe. The inferior olivary neurons belonging to the dorsal spino-olivo-cerebellar pathway are also monosynaptically activated by stimulation of the primary motor cortex (MI) and SI (Oscarsson, 1973). Mima et al. (1996, 1997) reported proprioception-related somatosensory evoked potentials (SEPs) from the scalp and epicortical recordings elicited by brisk passive flexion movement at the proximal interphalangeal joint of the middle finger (4° in 25 ms). Although the exact trigger point for eliciting the muscle afferents cannot be defined within the rise time (25 ms) of finger movement, they showed an early positivity with the peak latency of about 35 ms.

In the data by Kimura et al. (1999a,b), the onset latency of the first SI/MI response (P70 and P70m) was about 30 ms for pure muscle afferent inputs from the abductor pollicis brevis muscle. Thus it is possible that MI or SI activation elicits the third cerebellar response.

4.6. The fourth cerebellar activation reflects secondary activation of parallel fiber mediated Purkinje cell population

The fourth cerebellar activation with the latency of > 70 ms was present in all subjects for right MNS and in 2 out of 5 subjects for left MNS. The direction of the current was from the surface to the depth. The surface-sink and the depth-source field configuration suggests that the Purkinje cell population is activated by parallel fiber inputs. Further studies are needed to clarify the pathway mediating this late cerebellar response. The populations of neurons, which are candidates of successive responses, are schematically illustrated in Fig. 7.

4.7. Further studies are needed to bridge the gap between human MEG studies and electrophysiological studies in animals

Although the cerebellar responses are robust and reproducible in the majority of subjects, there are still some problems in the localization and timing of the cerebellar activation. First, there was no distinct ipsilateral activation of the intermediate zone for MNS as was shown in fMRI studies for hand movements. In addition, some of the activation foci were out of the cerebellum. Thus the localization from MEG data would need to be confirmed by another technique such as fMRI. With application of MNS and finger stimulation to the same group of subjects, the contribution of muscle afferents to the cerebellar responses can be verified by fMRI studies. Second, the timing of cerebellar signals was extremely variable among the subjects as compared with SI responses. We have no plausible explanation for the apparent discrepancy between the temporal properties of cerebellar and cerebral signals. Finally, one of the most serious problems in this study is the relation between the directions of intracellular current in a population of granule and Purkinje cells calculated from the MEG data and those in individual granule and Purkinje cell dendrites comprising the mass. The relation should be very complex and our present explanation of 'systematic asymmetry' in the cerebellar structure seems to be too simplistic. In order to approach the issue, an animal model would be preferable. For example, delivering the same stimulations to monkeys and measuring MEG signals from the monkey cerebellum and at the same time recording field- and extracellular unit-potentials from the cerebellar cortex, and the multimodal characterization of cerebellar activity can clarify the relation between the mass and local activities.

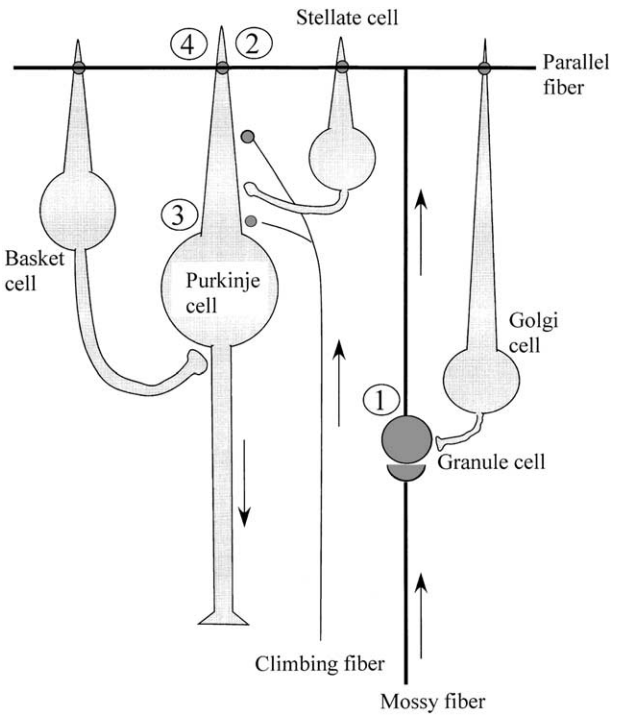

Fig. 7. The populations of neurons, which are candidates of successive responses, are illustrated on a schematic presentation of the main cell types and their synaptic arrangements in the cerebellar cortex. From the timing and current direction, we speculate that the 4 components reflect, respectively, (1) excitatory postsynaptic potentials (EPSPs) of granule cells, (2) Purkinje cell EPSPs at the distal dendrites driven by parallel fibers, (3) Purkinje cell EPSPs at the soma and the proximal dendrites mediated by climbing fibers and (4) second Purkinje cell EPSPs at the distal dendrites driven by parallel fibers. Black signifies excitatory transmission through climbing fibers, mossy fibers, granule cell and parallel fibers. The 3 kinds of inhibitory interneurons (Golgi cells, stellate cells and basket cells) are illustrated in gray. Although the granule cells are disynaptically inhibited by Golgi cells, and also Purkinje cells by stellate and basket cells, these inhibitory actions were not considered for simplicity. However, according to an animal study in cats by Murphy et al. (1973), only 3% of Purkinje cells were inhibited by the proprioceptive inputs. It is unknown what percentages of Purkinje cells were inhibited by the same inputs in humans. We infer that the percentages are not so much different between the two species.

Acknowledgements

We thank Gabriel Curio, Riitta Hari and Claudia D. Tesche for useful discussions, and Masato Taira for providing MRI data. The MR images were obtained at the First Department of Physiology, Nihon University School of Medicine.

References

Bell CC. Memory-based expectations in electrosensory systems. Curr Opin Neurobiol 2001;11:481–7.

Bushara KO, Wheat JM, Khan A, Mock BJ, Turski PA, Sorenson J, Brooks BR. Multiple tactile maps in the human cerebellum. Neuroreport 2001; 12:2483–6.

Eccles JC, Llinas R, Sasaki K. Parallel fibre stimulation and the responses induced thereby in the Purkinje cells of the cerebellum. Exp Brain Res 1966a;1:17–39.

Eccles JC, Llinas R, Sasaki K. The excitatory synaptic action of climbing fibres on the Purkinje cells of the cerebellum. J Physiol 1966b;182: 268–296.

Eccles JC, Provini L, Strata P, Taborikova H. Analysis of electrical potentials evoked in the cerebellar anterior lobe by stimulation of hindlimb and forelimb nerves. Exp Brain Res 1968;6:171–94.

Edin BB, Abbs JH. Finger movement responses of cutaneous mechanoreceptors in the dorsal skin of the human hand. J Neurophysiol 1991; 65:657–70.

Ellerman JM, Flament D, Kim S-G, Fu QG, Merkle H, Ebner TJ, Ugurbil K. Spatial patterns of functional activation of the cerebellum investigated using high field (4T) MRI. NMR Biomed 1994;7:63–8.

Ghez C, Thach WT. The cerebellum. In: Kandel E, Schwartz JH, Jessell TM, editors. Principles of neural science, 4th ed. New York: McGraw-Hill; 2000. p. 832–52.

Grafton SC, Woods RP, Mazziotta JC. Within arm somatotopy in human motor areas determined by positron emission tomography imaging of cerebral blood flow. Exp Brain Res 1993;95:172–6.

Grodd W, Hulsmann E, Lotze M, Wildgruber D, Erb M. Sensorimotor mapping of the human cerebellum: fMRI evidence of somatotopic organization. Hum Brain Mapp 2001;13:55–73.

Harvey RJ, Porter R, Rawson JA. The natural discharges of Purkinje cells in paravermal regions of lobules V and VI of the monkey's cerebellum. J Physiol 1977;271:515–36.

Hashimoto I. Somatosensory evoked potentials from the human brain-stem: origins of short latency potentials. Electroenceph clin Neurophysiol 1984;57:221–7.

Hashimoto I, Yoshikawa K, Sasaki M. Latencies of peripheral nerve and cerebral evoked responses to air-puff and electrical stimuli. Muscle Nerve 1990;13:1099–104.

Hashimoto I, Kimura T, Iguchi Y, Takino R, Sekihara K. Dynamic activation of distinct cytoarchitectonic areas of the human S1 cortex after median nerve stimulation. Neuroreport 2001a;12:1891–7.

Hashimoto I, Sakuma K, Kimura T, Iguchi Y, Sekihara K. Serial activation of distinct cytoarchitectonic areas of the human S1 cortex after posterior tibial nerve stimulation. Neuroreport 2001b;12:1857–62.

Ito M. The cerebellum and neural control. New York: Raven; 1984.

Katayama Y, Tsubokawa T. Somatosensory evoked potentials from the thalamic sensory relay nucleus (VPL) in human: correlations with short latency somatosensory evoked potentials recorded at the scalp. Electroenceph clin Neurophysiol 1987;68:187–201.

Kimura T, Nishijo K, Hashimoto I. Somatosensory evoked potentials elicited by motor point stimulation. In: Barber C, Celesia GG, Hashimoto I, Kakigi R, editors. Functional Neuroscience: Evoked Potentials and Magnetic Fields. EEG Suppl, 49. Amsterdam: Elsevier; 1999a. p. 73–6.

Kimura T, Nishijo K, Hashimoto I. Somatosensory evoked magnetic fields following motor point stimulation. In: Yoshimoto T, Kotani M, Kuriki S, Karibe H, Nakasato N, editors. Recent Advances in Biomagnetism. Sendai: Tohoku University Press; 1999b. p. 458–61.

Klostermann F, Gobbele R, Buchner H, Curio G. Intrathalamic non-propagating generators of high-frequency (1000 Hz) somatosensory evoked potential (SEP) bursts recorded subcortically in man. Clin Neurophysiol 2002;113:1001–5.

Lorente de No R. Action potential of the motoneurons of the hypoglossus nucleus. J Cell Comp Physiol 1947;29:207–87.

Mima T, Terada K, Maekawa M, Nagamine T, Ikeda A, Shibasaki H. Somatosensory evoked potentials following proprioceptive stimulation of finger in man. Exp Brain Res 1996;111:233–45.

Mima T, Ikeda A, Terada K, Yazawa S, Mikuni N, Kunieda T, Taki W, Kimura J, Shibasaki H. Modality-specific organization for cutaneous and proprioceptive sense in human primary sensory cortex studied by chronic epicortical recording. Electroenceph clin Neurophysiol 1997; 104:103–7.

Morioka T, Shima F, Kato M, Fukui M. Origin and distribution of thalamic somatosensory evoked potentials in humans. Electroenceph clin Neurophysiol 1989;74:186–93.

Murphy JT, MacKay WA, Johnson F. Differences between cerebellar mossy and climbing fibre responses to natural stimulation of forelimb muscle proprioceptors. Brain Res 1973;55:263–89.

Nitschke MF, Kleinschmidt A, Wessel K, Frahm J. Somatotopic motor representation in the human anterior cerebellum. A high-resolution functional MRI study. Brain 1996;119:1023–9.

Oldfield RC. The assessment and analysis of handedness: the Edinburgh inventory. Neuropsychologia 1971;9:97–113.

Okada YC, Nicholson C. Magnetic evoked field associated with transcortical currents in turtle cerebellum. Biophys J 1988;53:723–31.

Okada YC, Lauritzen M, Nicholson C. Magnetic field associated with neural activities in an isolated cerebellum. Brain Res 1987;412: 151–5.

Oscarsson O. Functional organization of spinocerebellar paths. In: Iggo A, editor. Somatosensory system. Handbook of sensory physiology, vol. 2. New York: Springer; 1973. p. 339–80.

Rushmer DS, Woollacott MH, Robertson LT, Laxter KD. Somatotopic organization of climbing fiber projections from low threshold cutaneous afferents to pars intermedia of cerebellar cortex in cat. Brain Res 1980; 181:17–30.

Sakai K, Takino R, Hikosaka O, Miyauchi S, Sasaki Y, Putz B, Fijimaki N. Separate cerebellar areas for motor control. Neuroreport 1998;9: 2359–63.

Sasaki K, Strata P. Responses evoked in the cerebellar cortex by stimulating mossy fiber pathways to the cerebellum. Exp Brain Res 1967;3:95–110.

Sekihara K, Nagarajan SS, Poeppel D, Marantz A, Miyashita Y. Reconstructing spatio-temporal activities of neural sources using an MEG vector beamformer technique. IEEE Trans Biomed Eng 2001;48: 760–71.

Sekihara K, Nagarajan SS, Robinson S, Vrba JY. Spatial resolution, leakage, and signal-to-noise ratio in adaptive beamformer source reconstruction technique. In: Nowak H, Haueisen J, Giessler F, Huonker R, editors. Proceedings of the 13th International Conference on Biomagnetism. Berlin: VDE; 2002. p. 813.

Sonoo M. How much has been solved regarding SEP generators? In: Barber C, Celesia GG, Hashimoto I,, Kakigi R, editors. Functional Neuroscience: Evoked Potentials and Magnetic Fields. EEG Suppl, 49. Amsterdam: Elsevier; 1999. p. 47–51.

Sonoo M, Genba K, Zai W, Iwata M, Mannen T, Kanazawa I. Origin of the widespread N18 in median nerve SEP. Electroenceph clin Neurophysiol 1992;84:418–25.

Tesche CD, Karhu J. Somatosensory evoked magnetic fields arising from sources in the human cerebellum. Brain Res 1997;744:23–31.

Tesche CD, Karhu J. Anticipatory cerebellar responses during somatosensory omission in man. Hum Brain Mapp 2000;9:119–42.

Thach WT. Correlation of neural discharge with pattern and force of muscular activity, joint position, and direction of intended next movement in motor cortex and cerebellum. J Neurophysiol 1978;41: 74–94.

Van Kan PLE, Houk JC, Gibson AR. Output organization of intermediate cerebellum of monkey. J Neurophysiol 1993a;69:57–73.

Van Kan PLE, Gibson AR, Houk JC. Movement-related inputs to intermediate cerebellum of the monkey. J Neurophysiol 1993b;69: 74–94.